

## Chapter 3

### Mathematical and Numerical Methodology

#### 3.1 Gas phase modeling

Several turbulence modeling techniques are used to handle the gas phase turbulence in this thesis: k-ε models that are in the framework of RANS model and a RNG-based LES model.

##### 3.1.1 General conservation equations for gas phase

CFD is fundamentally based on the governing equations of fluid dynamics. They represent mathematical statements of the conservation laws of physics. These laws have been derived from the fact that certain measures must be conserved in a particular volume, which is called control volume. The gas phase conservation equations of a scalar  $\Phi$  can be cast in a general form:

$$\frac{\partial(\rho_g \phi)}{\partial t} + \frac{\partial(\rho_g u_i^g)}{\partial x_j} = \frac{\partial}{\partial x_j} \left( \Gamma \frac{\partial \phi}{\partial x_j} \right) + q_\phi \quad (3.1)$$

(1)            (2)            (3)            (4)

where  $t$  is time and  $u_i^g$  represents gas velocity.  $\Gamma$  is the diffusivity of the scalar and  $q_\phi$  is a general source term. The term (1) in Equation (3.1) is the local acceleration term and term (2) is the advection term. The term (3) on the right hand side is the diffusion term and term (4) is the source term.

This equation is usually used as the starting point for computational procedures in either the finite difference or finite volume methods. Algebraic expressions of this equation for the various transport properties are formulated and hereafter solved. By setting the transport property  $\phi$  equal to 1,  $u_g$ ,  $T$ , and selecting appropriate values for the diffusion coefficient  $\Gamma$  and source terms  $q_\phi$ , one can obtain the special forms presented in Table 3.1 for each of the partial differential equations for the conservation of mass, momentum and

energy.

**Table 3.1** The Governing Equations for Gas phase in Cartesian Coordinates

**Conservation of mass** ( $\phi = 1$ )

$$\frac{\partial \rho_g}{\partial t} + \frac{\partial(\rho_g u_j^g)}{x_j} = 0 \quad (3.2)$$

For incompressible flow

$$\frac{\partial(\rho_g u_j^g)}{x_j} = 0$$

**Conservation of Momentum** ( $\phi = u_i^g$ )

$$\frac{\partial(\rho_g u_i^g)}{\partial t} + \frac{\partial(\rho_g u_j^g u_i^g)}{\partial x_j} = \frac{\partial}{\partial x_j} \left( \mu_g \frac{\partial u_i^g}{\partial x_j} \right) - \frac{\partial p_g}{\partial x_i} \quad (3.3)$$

**Energy Equation** ( $\phi = T$ )

$$\frac{\partial(\rho_g T)}{\partial t} + \frac{\partial(\rho_g u_j^g T)}{\partial x_j} = \frac{\partial}{\partial x_j} \left( \frac{\mu_g}{\text{Pr}} \frac{\partial T}{\partial x_j} \right) \quad (3.4)$$

### 3.1.2 k-ε models

Many engineering applications require computational procedure that can supply adequate information about the time-averaged properties of the flow (such as mean velocities, mean pressures, mean stresses etc.), but which avoid the need to predict all the effects associated with each and every eddy in the flow. Therefore, by adopting a suitable time-averaging operation on the momentum equations, one is able to discard all details concerning the state of the flow contained in the instantaneous fluctuations. Osborne Reynolds first

introduced the notation of splitting the instantaneous flow variables into their mean and fluctuating components (Hinze, 1975):

$$\phi(x_i, t) = \bar{\phi}(x_i) + \phi'(x_i, t) \quad (3.5)$$

Note that the overbar in Equation (3.5) denotes the time-averaged qualities. For an incompressible fluid, this process that is performed on the continuity Equation (3.2) and the conservation form of momentum Equations (3.3) produces the time-averaged governing equations or more popularly known as the RANS equations:

$$\frac{\partial(\rho_g \bar{u}_j^g)}{\partial x_j} = 0 \quad (3.6)$$

$$\frac{\partial(\rho_g \bar{u}_i^g)}{\partial t} + \frac{\partial(\rho_g \bar{u}_j^g \bar{u}_i^g)}{\partial x_j} = \frac{\partial}{\partial x_j} \left( \mu_g \frac{\partial \bar{u}_i^g}{\partial x_j} \right) - \frac{\partial \bar{p}_g}{\partial x_i} - \frac{\partial(\rho_g \overline{u'_i u'_j})}{\partial x_j} + \frac{\partial \bar{\tau}_{ij}}{\partial x_j} \quad (3.7)$$

where  $\bar{u}_i^g$  and  $u'_i$  are gas phase mean velocity and gas phase fluctuating velocity, respectively. The  $\bar{\tau}_{ij}$  are the mean viscous stress tensor components:

$$\bar{\tau}_{ij} = \mu_g \left( \frac{\partial \bar{u}_i^g}{\partial x_j} + \frac{\partial \bar{u}_j^g}{\partial x_i} \right) \quad (3.8)$$

The time-averaged equations can be solved if the unknown Reynolds stresses,  $\rho_g \overline{u'_i u'_j}$  in Equation (3.7) can be related to the mean flow quantities. It was proposed that the Reynolds stresses could be linked to the mean rates of deformation (Hinze, 1975):

$$\rho_g \overline{u'_i u'_j} = \mu_{g,t} \left( \frac{\partial \bar{u}_i^g}{\partial x_j} + \frac{\partial \bar{u}_j^g}{\partial x_i} \right) - \frac{2}{3} \rho_g \sigma_{ij} k_g \quad (3.9)$$

where  $\mu_{g,t}$  is the eddy viscosity or turbulent viscosity.

Since the complexity of turbulence in most engineering flow problems precludes the use of any simple formulae, it is possible to develop similar transport equations to accommodate the turbulent quantity  $k_g$  and other turbulent quantities such as the rate of dissipation of turbulent energy  $\epsilon_g$ . Here,  $k_g$  be defined and expressed in Cartesian tensor notation as:

$$k_g = \frac{1}{2} \overline{u'_i u'_i} \quad (3.10)$$

and  $\epsilon_g$

$$\epsilon_g = \frac{\mu_{g,t}}{\rho_g} \overline{\left( \frac{\partial u'_i}{\partial x_j} \right) \left( \frac{\partial u'_i}{\partial x_j} \right)} \quad (3.11)$$

From the local values of  $k_g$  and  $\epsilon_g$ , a local turbulent viscosity  $\mu_{g,t}$  can be evaluated as:

$$\mu_{g,t} = \frac{C_\mu \rho_g k_g^2}{\epsilon_g} \quad (3.12)$$

By substituting the Reynolds stress expressions in Equation (3.9) into the governing Equation (3.6) and (3.7), and removing the overbar that is indicating the time-averaged quantities, one obtains the following equations:

$$\frac{\partial(\rho_g u_j^g)}{\partial x_j} = 0 \quad (3.13)$$

$$\frac{\partial(\rho_g u_i^g)}{\partial t} + \frac{\partial}{\partial x_j} \left( \rho_g u_i^g u_j^g - (\mu_{g,t} + \mu_g) \left( \frac{\partial u_i^g}{\partial x_j} + \frac{\partial u_j^g}{\partial x_i} \right) \right) = -\frac{\partial p_g}{\partial x_i} \quad (3.14)$$

The additional differential transport equations that is required for the standard k- $\epsilon$  model, which for the case of a constant fluid property and expressed in non-conservation form are:

$$\frac{\partial(\rho_g k_g)}{\partial t} + \frac{\partial(\rho_g u_j^g k_g)}{\partial x_j} = \frac{\partial}{\partial x_j} \left( \left( \mu_g + \frac{\mu_{g,t}}{\sigma_k} \right) \frac{\partial k_g}{\partial x_j} \right) - \rho_g \overline{u'_i u'_j} \frac{\partial u_i^g}{\partial x_j} - \rho_g \epsilon_g \quad (3.15)$$

here, the rate of production of turbulent kinetic energy  $P_k = -\rho_g \overline{u'_i u'_j} \frac{\partial u_i^g}{\partial x_j}$  can be modelled by:

$$-\rho_g \overline{u'_i u'_j} \frac{\partial u_i^g}{\partial x_j} \approx \mu_{g,t} \left( \frac{\partial u_i^g}{\partial x_j} + \frac{\partial u_j^g}{\partial x_i} \right) \frac{\partial u_i^g}{\partial x_j} \quad (3.16)$$

and

$$\frac{\partial(\rho_g \epsilon_g)}{\partial t} + \frac{\partial(\rho_g u_j^g \epsilon_g)}{\partial x_j} = \frac{\partial}{\partial x_j} \left( \left( \mu_g + \frac{\mu_{g,t}}{\sigma_\epsilon} \right) \frac{\partial \epsilon_g}{\partial x_j} \right) - C_{1\epsilon} \frac{\epsilon_g}{k_g} P_k - \rho_g C_{2\epsilon} \frac{\epsilon_g^2}{k_g} \quad (3.17)$$

The equations contain five adjustable constants  $C_\mu$ ,  $\sigma_k$ ,  $\sigma_\epsilon$ ,  $C_{1\epsilon}$  and  $C_{2\epsilon}$ . These constants have been arrived at by comprehensive data fitting for a wide range of turbulent flows (Launder and Spalding, 1974):

$$C_\mu = 0.09, \quad \sigma_k = 1.0, \quad \sigma_\epsilon = 1.3, \quad C_{1\epsilon} = 1.44, \quad C_{2\epsilon} = 1.92.$$

Yakhot et al. (1984) developed a k- $\epsilon$  model based on the Re-Normalization Group (RNG) theory. The transport equations for  $k$  and  $\epsilon$  are given as following:

$$\frac{\partial(\rho_g k_g)}{\partial t} + \frac{\partial(\rho_g u_j^g k_g)}{\partial x_j} = \frac{\partial}{\partial x_j} \left( \sigma_k \mu_{eff} \frac{\partial k_g}{\partial x_j} \right) + P_k - \rho_g \epsilon_g \quad (3.18)$$

$$\frac{\partial(\rho_g \epsilon_g)}{\partial t} + \frac{\partial(\rho_g u_j^g \epsilon_g)}{\partial x_j} = \frac{\partial}{\partial x_j} \left( \sigma_\epsilon \mu_{eff} \frac{\partial \epsilon_g}{\partial x_j} \right) - C_{1\epsilon} \frac{\epsilon_g}{k_g} P_k - \rho_g C_{2\epsilon} \frac{\epsilon_g^2}{k_g} - R \quad (3.19)$$

One of difference between the standard and RNG turbulence models is the turbulent viscosity. The scale elimination procedure in RNG theory results in a differential equation for turbulent viscosity  $\mu_{eff}$ :

$$d\left(\frac{\rho_g^2 k_g}{\sqrt{\epsilon_g \mu_g}}\right) = 1.72 \frac{\hat{v}}{\sqrt{\hat{v}^3 - 1 + C_v}} d\hat{v} \quad (3.20)$$

where  $\hat{v} = \mu_{eff} / \mu_g$  and  $C_v = 100$ .

Another difference between the standard and RNG k- $\epsilon$  models is the presence of an additional strain rate term  $R$  in the  $\epsilon$ -equation (3.19) for the RNG k- $\epsilon$  model. The term is modeled as:

$$R = \frac{C_\mu \eta^3 (1 - \eta/\eta_o) \epsilon_g^2}{1 + \beta \eta^3} \frac{1}{k_g} \quad (3.21)$$

Here,  $\beta$  and  $\eta_o$  are constants with values of 0.015 and 4.38. The significance of the inclusion of this term is its responsiveness towards the effects of rapid rate strain and streamlines curvature, which cannot be properly represented by the standard k- $\epsilon$  model. According to the RNG theory, the constants in the turbulent transport equations are given by  $\sigma_k = 0.718$ ,  $\sigma_\epsilon = 0.718$ ,  $C_{1\epsilon} = 1.42$  and  $C_{2\epsilon} = 1.68$  respectively (Yakhot et al., 1984).

The realizable k- $\epsilon$  model proposed by Shih et al. (1995) is intended to address deficiencies experienced in the standard and RNG k- $\epsilon$  models. The term “realizable” means that the model satisfies certain mathematical constraints on the normal stresses, consistent with the physics of turbulent flows. The k-equation is the same as that in the standard k- $\epsilon$  model except for model constants. The development involved the formulation of a new eddy-viscosity formula involving the variable  $C_\mu$  in the turbulent viscosity relationship (Equation (3.12)) and a new model for the  $\epsilon$ -equation based on the dynamic equation of the mean-square vorticity fluctuation. The following are the  $k_g$  and  $\epsilon_g$  transport equations for the realizable k- $\epsilon$  model:

$$\frac{\partial(\rho_g k_g)}{\partial t} + \frac{\partial(\rho_g u_j^g k_g)}{\partial x_j} = \frac{\partial}{\partial x_j} \left( \left( \mu_g + \frac{\mu_{g,t}}{\sigma_k} \right) \frac{\partial k_g}{\partial x_j} \right) + p_k - \rho_g \epsilon_g \quad (3.22)$$

$$\frac{\partial(\rho_g \varepsilon_g)}{\partial t} + \frac{\partial(\rho_g u_j^g \varepsilon_g)}{\partial x_j} = \frac{\partial}{\partial x_j} \left( \left( \mu_g + \frac{\mu_{g,t}}{\sigma_k} \right) \frac{\partial \varepsilon_g}{\partial x_j} \right) + \rho_g C_1 S \varepsilon_g - \rho_g C_2 \frac{\varepsilon_g^2}{k_g + \sqrt{\frac{\mu_g \varepsilon_g}{\rho_g}}} \quad (3.23)$$

where  $S$  is the mean strain rate  $S = \sqrt{2S_{ij}S_{ij}}$ . The variable  $C_1$  can be expressed as:

$$C_1 = \max \left[ 0.43, \frac{\eta}{\eta + 5} \right] \text{ and } \eta = \frac{\kappa_g}{\varepsilon_g} (2S_{ij}S_{ij})^{1/2} \quad (3.24)$$

The variable  $C_\mu$ , no longer a constant, is computed from:

$$C_\mu = \frac{1}{A_0 + A_s \frac{k_g U^*}{\varepsilon_g}}; \quad U^* \equiv \sqrt{S_{ij}S_{ij} + \tilde{\Omega}_{ij}\tilde{\Omega}_{ij}}; \quad \tilde{\Omega}_{ij} = \Omega_{ij} - 2\varepsilon_{ijk}\omega_k; \quad \Omega_{ij} = \bar{\Omega}_{ij} - \varepsilon_{ijk}\omega_k \quad (3.25)$$

while the model constant  $A_0$  and  $A_s$  are determined by:

$$A_0 = 4.04; \quad A_s = \sqrt{6} \cos \varphi; \quad \varphi = \frac{1}{3} \cos^{-1}(\sqrt{6}W); \quad W = \frac{S_{ij}S_{jk}S_{ki}}{S^3}; \quad S = \sqrt{S_{ij}S_{ij}} \quad (3.26)$$

Other constants in the turbulent transport equations are given to be  $C_2 = 1.9$ ,  $\sigma_k = 1.0$  and  $\sigma_\varepsilon = 1.2$  respectively (Shih et al., 1995).

### 3.1.3 RNG-based LES model

In LES models, the small eddies are separated by filters from large eddies that contain most of the energy. The resulting equations thus resolve only the dynamics of large eddies and these large-scale variables that can be achieved by the filtering operation:

$$\bar{f}(x) = \frac{1}{\Delta V} \int f(x') dx' \quad (3.27)$$

Here,  $\Delta V$  is the control volume (the finite-volume cell). Applying the filtering operation to the conservation equations, the governing equations for the large-scale variables are:

$$\frac{\partial \rho_g}{\partial t} + \frac{\partial}{\partial x_i} (\rho_g \bar{u}_i^g) = 0 \quad (3.28)$$

$$\frac{\partial}{\partial t} (\rho_g \bar{u}_i^g) + \frac{\partial}{\partial x_j} (\rho_g \bar{u}_j^g \bar{u}_i^g) = \frac{\partial}{\partial x_j} \left( \mu_g \frac{\partial \bar{u}_i^g}{\partial x_j} \right) - \frac{\partial p_g}{\partial x_i} - \frac{\partial \tau_{ij}}{\partial x_j} \quad (3.29)$$

where  $\bar{u}_g$  is the resolved gas phase velocity. That is different from the overbar in RANS modeling techniques (equation 3.6, 3.7), where it represents the Reynolds-averaged quantities. The effect of the small scales upon the resolved part of turbulence appears in the SGS stress term:  $\tau_{ij} = \rho_g \overline{u_j^g u_i^g} - \rho_g \bar{u}_j^g \bar{u}_i^g$ . Yakhot et al. (1989) derived a subgrid model by applying the RNG theory to the SGS eddy viscosity. In this RNG-based SGS model, the stress is modelled according to:

$$\tau_{ij} - \frac{\delta_{ij}}{3} \tau_{kk} = 2\mu_{eff}^s \bar{S}_{ij} \quad (3.30)$$

Here,  $\mu_{eff}^s$  is the SGS turbulent viscosity given as:

$$\mu_{eff}^s = \mu_g [1 + H(x)]^{1/3} \quad (3.31)$$

$H(x)$  is the ramp function defined by:

$$H(x) = \begin{cases} x, & x \geq 0 \\ 0, & x < 0 \end{cases} \quad (3.32)$$

where,  $x$  equals to  $\frac{\mu_s^2 \mu_{eff}^s}{\mu_g^3} - C$ .  $\mu_s = (C_{RNG} \Delta V^{1/3})^2 \sqrt{2\bar{S}_{ij} \bar{S}_{ij}}$ . Based on the RNG theory,

the constants  $C_{RNG}$  and  $C$  are 0.157 and 100, respectively.



## 3.2 Particle phase modeling

### 3.2.1 Eulerian-Eulerian model

The Eulerian-Eulerian model developed by Tu and Fletcher (1995) and Tu (1997) was employed in this study. The RNG  $k$ - $\varepsilon$  model was used to handle the gas-phase turbulence. And a two-way coupling was achieved between the continuum gas and particle phase. For the confined two-phase flow, the two-way coupling effects of the particle phase on the turbulence of the gas phase are accounted through additional source terms in the  $k_g$  and  $\varepsilon_g$  equations:

$$S_{\text{add}}^k = \frac{2f}{t_p} \rho_p (k_g - k_{gp}) \quad (3.33)$$

in the  $k_g$  equation and

$$S_{\text{add}}^\varepsilon = \frac{2f}{t_p} \rho_p (\varepsilon_g - \varepsilon_{gp}) \quad (3.34)$$

in the  $\varepsilon_g$  equation, where  $k_{gp}$  and  $\varepsilon_{gp}$  are provided below from the particle turbulence model and  $f$  is the correction factor selected from Schuh et al. (1989).

The particle phase conservation equations are expressed by:

Continuity equation:

$$\frac{\partial}{\partial x_i} (\rho_p u_i^p) = 0 \quad (3.35)$$

Momentum equation:

$$\frac{\partial}{\partial x_j} (\rho_p u_j^p u_i^p) = - \frac{\partial}{\partial x_j} (\rho_p \overline{u_j'^p u_i'^p}) + F_{Gi} + F_{Di} + F_{WMi} \quad (3.36)$$

Particle turbulent fluctuating energy equation:

$$\frac{\partial}{\partial x_j} (\rho_p u_j^p k_p) = \frac{\partial}{\partial x_j} (\rho_p \frac{\nu_{p,t}}{\sigma_p} \frac{\partial k_p}{\partial x_j}) + P_{kp} - I_{gp} \quad (3.37)$$

Gas particle correlation equation:

$$\frac{\partial}{\partial x_j} [\rho_p (u_j^g + u_j^p) k_{gp}] = \frac{\partial}{\partial x_j} \rho_p (\frac{\nu_{g,t}}{\sigma_g} + \frac{\nu_{p,t}}{\sigma_p}) \frac{\partial k_{gp}}{\partial x_j} + P_{jgp} - \rho_p \epsilon_{gp} - \Pi_{gp} \quad (3.38)$$

The forces  $F_{Di}$ ,  $F_{Gi}$  and  $F_{WMi}$  are the Favre-averaged aerodynamic drag, gravity and wall-momentum transfer due to particle-wall collision respectively. The aerodynamic force  $F_{Di}$  due to the slip velocity between the two phases is given by:

$$F_{Di} = \rho_p \frac{f(u_i^g - u_i^p)}{\tau_p} \quad (3.39)$$

The turbulent viscosity of the particle phase is computed through the following relationship:

$$\nu_{p,t} = 1_{p,t} \sqrt{\frac{2}{3}} k_p \quad (3.40)$$

The characteristic length  $l_{p,t}$  is obtained by:  $l_{p,t} = \min(l'_{p,t}, L_s)$  with  $l'_{p,t}$  is given as:

$$l'_{p,t} = \frac{l_{g,t}}{2} (1 + \cos^2 \theta) \exp \left[ -B_{gp} \frac{|u'_r|}{|u'_g|} \text{sign}(k_g - k_p) \right] \quad (3.41)$$

The characteristic length of the system  $L_s$  provides a limit to the characteristic length of the particle phase. In Equation (3.41),  $\theta$  denotes the angle between the velocity of the particle and velocity of the gas to account for the crossing trajectories effect (Huang, 1993) while  $B_{gp}$  denotes a constant determined experimentally, which yields a value of 0.01. The relative fluctuating velocity in Equation (3.41) can be written as:

$$u'_r = u'_g - u'_p \quad (3.42)$$

Applying the modulus on Equation (3.42) yields the following:

$$|u'_r| = \sqrt{u'^2_g - 2u'_g u'_p + u'^2_p} = \sqrt{\frac{2}{3}(k_p - 2k_{pg} + k_g)} \quad (3.43)$$

The turbulent Prandtl-Schmidt number  $\sigma_p$  for the particle turbulent fluctuating energy (Equation (3.38)) has a value of 0.7179. The turbulence production of the particle phase is formulated as:

$$P_{kp} = \rho_p \nu_{p,t} \left( \frac{\partial u_i^p}{\partial x_j} + \frac{\partial u_j^p}{\partial x_i} \right) \frac{\partial u_i^p}{\partial x_j} - \frac{2}{3} \rho_p \delta_{ij} \left( \kappa + \nu_{p,t} \frac{\partial u_k^p}{\partial x_k} \right) \frac{\partial u_i^p}{\partial x_j} \quad (3.44)$$

while the turbulence interaction between the gas and particle phases is:

$$I_{gp} = \frac{2f}{t_p} \rho_p (k_g - k_{gp}) \quad (3.45)$$

The turbulence production by the mean velocity gradients of two phases is given by:

$$P_{kp} = \left[ \rho_p \left( v_{g,t} \frac{\partial u_i^g}{\partial x_j} + v_{p,t} \frac{\partial u_j^p}{\partial x_i} \right) - \frac{2}{3} \rho_p \delta_{ij} \kappa_{gp} - \frac{1}{3} \rho_p \delta_{ij} \left( v_{g,t} \frac{\partial u_k^p}{\partial x_k} + v_{p,t} \frac{\partial u_k^p}{\partial x_k} \right) \right] \left( \frac{\partial u_k^g}{\partial x_j} + v_{p,t} \frac{\partial u_j^p}{\partial x_i} \right) \quad (3.46)$$

while the interaction term between the two phases yields:

$$\Pi_{gp} = \frac{f}{2t_p} \rho_p [(1+m)2k_{gp} - 2k_g - m2k_p] \quad (3.47)$$

Here,  $m$  is the ratio of particle to gas density,  $m = \rho_p/\rho_g$ . The dissipation term due to the gas viscous effect is given as:

$$\epsilon_{gp} = \epsilon_g \exp \left( -B_\epsilon t_p \frac{\epsilon_g}{\kappa_g} \right) \quad (3.48)$$

where  $B_\epsilon = 0.4$ .

The particle boundary conditions at the solid wall were consistent with the Lagrangian description. For Lagrangian treatment, the rebound velocity components of the individual particles can be described as:

$$\begin{aligned} v_n^{p,L} &= -e_n u_n^{p,L} \\ v_t^{p,L} &= e_t u_t^{p,L} \end{aligned} \quad (3.49)$$

where the subscripts n and t denote the normal and tangential directions. The superscript L denotes the Lagrangian quantity. In order to derive the Eulerian formulation of boundary conditions for the particle phase, a finite control volume adjacent to the wall surface is considered (Figure 3.1) and the following assumptions are made (Tu and Fletcher, 1995):

- (1) The length of the control volume is much larger than the height, i.e.  $L \gg h$ .
- (2) Incident particles at the top of control volume arrive with different velocities and directions.
- (3) Due to the wall surface roughness, reflected particles arrive at the top surface from underneath with different velocities and directions.
- (4) The flow is steady.

The mean particle rebounding velocity components can be expressed approximately by the mean restitution coefficients (  $\bar{e}_n$  and  $\bar{e}_t$  ) and average velocities with Lagrangian components (incident and reflected parts):

$$\bar{v}_{n,h}^{p,L} = -\bar{e}_n \bar{u}_{n,h}^{p,L} \quad (3.50a)$$

$$\bar{v}_{t,h}^{p,L} = \bar{e}_t \bar{u}_{t,h}^{p,L} \quad (3.50b)$$

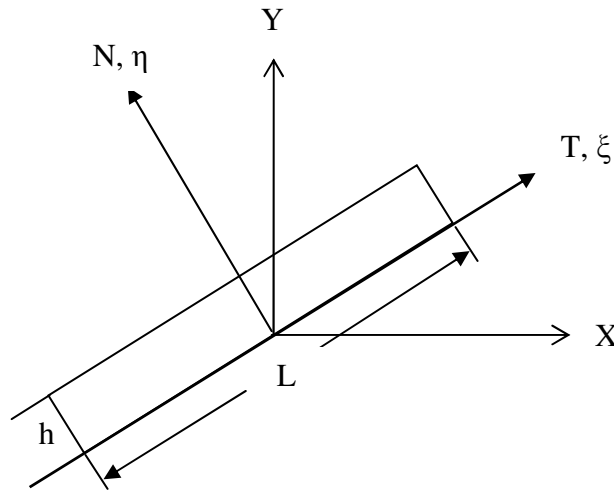


**Figure 3.1** A finite control volume adjacent to a solid wall for deriving wall boundary conditions of particle phase

for steady flow, when imposing the mass conservation for the control volume and exploiting assumption 1, the following equation is obtained:

$$N_i^p \left| \bar{u}_{n,h}^{p,L} \right| - N_r^p \left| \bar{v}_{n,h}^{p,L} \right| = 0 \quad (3.51)$$

and:

$$N = N_i^p + N_r^p, \quad n_i^p = N_i^p / N, \quad n_r^p = 1 - n_i^p \quad (3.52)$$

where  $N_i^p$  is the number of incoming particles per volume arriving in the control volume and  $N_r^p$  the number of reflected particles per volume leaving the control volume. From Equation (3.50a) and Equation (3.51) one can obtain the following equation:

$$n_i^p / n_r^p = \bar{e}_n \quad (3.53)$$

And with Equation (3.52), one can have:

$$\begin{aligned} \bar{e}_n &= n_i^p / (1 - n_i^p) \\ n_i^p &= \bar{e}_n / (1 + \bar{e}_n) \end{aligned} \quad (3.54)$$

The Eulerian quantities can be connected with Lagrangian quantities (incident and reflected parts) at the top of the control volume

$$\left( N \left| \bar{u}_{n,h}^{p,E} \right| A_n \right) \left( \bar{u}_{n,h}^{p,E} \right)^q = \left( N_i^p \left| \bar{u}_{n,h}^{p,L} \right| A_n \right) \left( \bar{u}_{n,h}^{p,L} \right)^q + \left( N_r^p \left| \bar{v}_{n,h}^{p,L} \right| A_n \right) \left( \bar{v}_{n,h}^{p,L} \right)^q \quad (3.55a)$$

$$\left(\bar{u}_{n,h}^{p,E}\right)^{q+1} = \left(\bar{u}_{n,h}^{p,L}\right)^{q+1} n_i^p \left[1 + \left(n_r^p / n_i^p\right) (\bar{e}_n)(-\bar{e}_n)^q\right] \quad (3.55b)$$

where the superscript E denotes the Eulerian average quantity. As  $\left|\bar{v}_{n,h}^{p,L}\right| \leq \left|\bar{u}_{n,h}^{p,L}\right|$  when  $\bar{e}_n \leq 1$ ,  $\bar{u}_{n,h}^{p,E}$  is in the same direction with  $\bar{v}_{n,h}^{p,L}$ . From Equation (3.50a), (3.53) and (3.54), one can get:

$$\bar{u}_{n,h}^{p,E} = \bar{u}_{n,h}^{p,L} B^N \text{ and } B^N = \left( \frac{\bar{e}_n [1.0 + (-\bar{e}_n)^q]}{1.0 + \bar{e}_n} \right)^{1/(q+1)} \quad (3.56)$$

where q is a factor required for the averaging process,  $1 \leq q \leq 2$ .  $q=1$  refers to a momentum average and  $q=2$  corresponds to an energy average. An equivalent formula to Equation (3.55b) applies to the tangential component of velocity and, using (3.30b), (3.53) and (3.54), one obtains:

$$\bar{u}_{t,h}^{p,E} = \bar{u}_{t,h}^{p,L} B^T \text{ and } B^T = \left( \frac{\bar{e}_n + (\bar{e}_t)^{q+1}}{1.0 + \bar{e}_p} \right)^{1/(q+1)} \quad (3.57)$$

by analogy to the flow of gas molecules, the normal and tangential Eulerian velocities of the particle phase at  $\eta = h$  from the wall surface can be linked to the Eulerian solution at  $\eta = 0$  using a Taylor's expansion:

$$\bar{u}_{n,h}^{p,E} \approx \bar{u}_{n,w}^{p,E} + h \left[ \frac{\partial \bar{u}_n^{p,E}}{\partial \eta} \right] \quad (3.58a)$$

$$\bar{u}_{t,h}^{p,E} \approx \bar{u}_{t,w}^{p,E} + h \left[ \frac{\partial \bar{u}_t^{p,E}}{\partial \eta} \right] \quad (3.58b)$$

At the wall the equivalent of Equation (3.55a) is used to link the Eulerian and Lagrangian solution, except that  $n_r^p = n_i^p = 0.5$  for the steady flow:

$$\bar{u}_{n,w}^{p,E} = \bar{u}_{n,w}^{p,L} A^N \quad \text{and} \quad A^N = \left( \frac{1.0 + \bar{e}_n (-\bar{e}_n)^q}{2.0} \right)^{1/(q+1)} \quad (3.59)$$

and:

$$\bar{u}_{t,w}^{p,E} = \bar{u}_{t,w}^{p,L} A^T \quad \text{and} \quad A^T = \left( \frac{1.0 + (\bar{e}_t)^{q+1}}{2.0} \right)^{1/(q+1)} \quad (3.60)$$

One can link the Lagrangian solution at  $\eta = h$  with the Lagrangian solution at  $\eta = 0$  and assume:

$$\bar{u}_{n,h}^{p,L} \approx \bar{u}_{n,w}^{p,L} \quad \text{and} \quad \bar{u}_{t,h}^{p,L} \approx \bar{u}_{t,w}^{p,L} \quad (3.61)$$

Equation (3.61) is a good approximation for high inertia particles. For low inertial particles, a local Knudsen number  $Kn$  which is defined by a gas-particle interaction length,  $l_{gp}$ , divided by the system characteristics length,  $l_s$ , to connect to the change due to the aerodynamic drag between  $\eta = 0$  and  $\eta = h$ . For turbulent flow,  $l_{gp} = t_p |W_R'|$  as defined by Soo where  $|W_R'|$  is the modulus of the relative turbulence intensity. Herein, the slip velocity  $|W_R|$  is taken instead of the relative turbulence. Then, one can use  $Kn_h = h(l_{gp}/D) = hKn$  to replace  $h$  in Equation (3.58) (where  $Kn_h < h$ , i.e. when  $Kn$  is larger than unity, it can be imposed that  $Kn_h = 1$  because it is just adjusted for low inertial particles). Combining Equations from (3.56) to (3.61), one obtains:



$$(A^N - B^N)\bar{u}_{n,w}^{p,E} + A^N Kn_h \left[ \frac{\partial \bar{u}_n^{p,E}}{\partial \eta} \right]_w = 0 \quad (3.62)$$

$$(A^T - B^T)\bar{u}_{t,w}^{p,E} + A^T Kn_h \left[ \frac{\partial \bar{u}_t^{p,E}}{\partial \eta} \right]_w = 0 \quad (3.63)$$

The condition of zero mass flux at the wall may be written as:

$$\left[ \frac{\partial(\rho_p \bar{u}_n^{p,E})}{\partial \eta} \right]_w = \rho_{p,w} \left[ \frac{\partial(\bar{u}_n^{p,E})}{\partial \eta} \right]_w + \bar{u}_{n,w}^{p,E} \left[ \frac{\partial(\rho_p)}{\partial \eta} \right]_w = 0 \quad (3.64)$$

From Equation (3.62) and (3.64) one obtains:

$$(B^N - A^N)\rho_{p,w} + A^N Kn_h \left[ \frac{\partial \rho_p}{\partial \eta} \right]_w = 0 \quad (3.65)$$

Therefore, the generalized wall boundary conditions for the particle phase can be written in a generic form:

$$a\phi_w + b \left[ \frac{\partial \phi}{\partial \eta} \right]_w = c, \quad \phi = [\bar{u}_n^{p,E}, \bar{u}_t^{p,E}, \rho_p] \quad (3.66)$$

The coefficients in the equation are:

$$\begin{aligned} a_N &= A^N - B^N; & b_N &= A^N Kn_h; & c_N &= 0 \\ a_T &= A^T - B^T; & b_T &= A^T Kn_h; & c_T &= 0 \\ a_\rho &= B^N - A^N; & b_\rho &= A^N Kn_h; & c_\rho &= 0 \end{aligned} \quad (3.67)$$

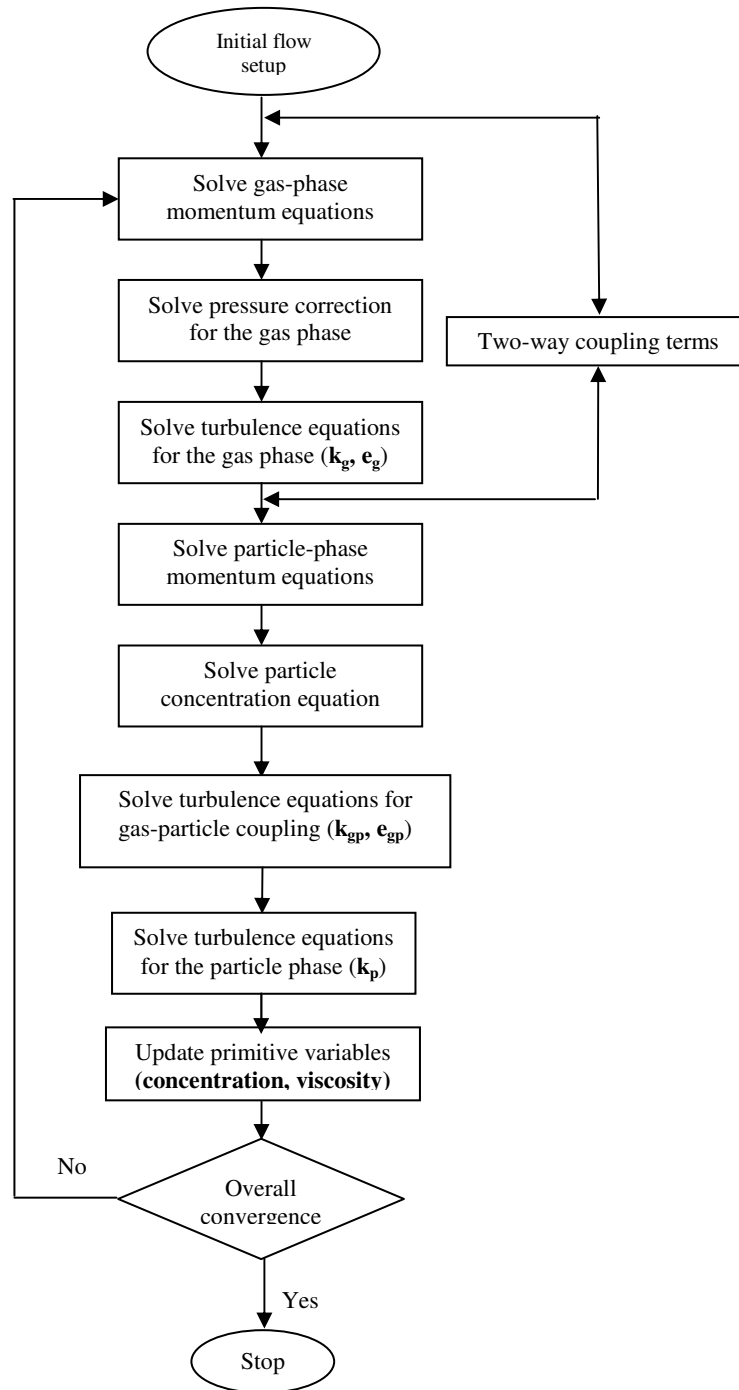


**Figure 3.2** Solution procedures for Eulerian two-fluid model

In the Eulerian model, all the governing equations for both gas and particle phase are solved sequentially at each iteration, this has been depicted with the aid of a flow chart (Figure 3.2). The solution process starts by solving the momentum equations of the gas phase followed by the pressure-correction through continuity. This is then followed by

solution of turbulence equations for the gas phase, whereas the solution process for the particle phase starts by solving the momentum equations followed by the concentration and then by the gas-particle turbulence interaction and ends by solving the turbulence equation for the particulate phase. At each global iteration, each equation is iterated, typically 3 to 5 times, using a strongly implicit procedure (SIP). The above solution process is marched towards a steady state and is repeated until a converged solution is obtained.

### 3.2.2 Eulerian-Lagrangian model

A Lagrangian-formulated particle equation of motion is solved using FLUENT. The trajectory of a discrete particle phase is determined by integrating the force balance on the particle. This force balance equates the particle inertia with the forces acting on the particle. Appropriate forces such as the drag and gravitational forces have been incorporated into the equation of motion. The equation can be written as

$$\frac{du_p}{dt} = F_D(u_g - u_p) + \frac{g(\rho_p - \rho_g)}{\rho_p} \quad (3.68)$$

where  $F_D(u_g - u_p)$  is the drag force per unit particle mass, and  $F_D$  is given by:

$$F_D = \frac{18\mu_g C_D \text{Re}_p}{24\rho_p d_p^2} \quad (3.69)$$

where  $\rho_p$  denotes the density of particle material and  $d_p$  is the particle diameter.  $u_p$  presents the particle velocity.  $\text{Re}_p$  is the relative Reynolds number defined as:

$$\text{Re}_p = \frac{\rho_g d_p |u_p - u_g|}{\mu_g} \quad (3.70)$$

The drag coefficient ( $C_D$ ) is correlated as a function of the  $\text{Re}_p$ :

$$C_D = \begin{cases} 0.44 & \text{Re}_p > 1000 \\ \frac{24}{\text{Re}_p} \left( 1.0 + \frac{1}{6} \text{Re}_p^{0.66} \right) & \text{Re}_p < 1000 \end{cases} \quad (3.71)$$

The CFD code, FLUENT, handles the turbulent dispersion of particles by integrating the trajectory equations for individual particles, using the instantaneous fluid velocity,  $u^g + u'(t)$ , along the particle path during the integration process. Here, a stochastic method, discrete random walk or “eddy lifetime” model, is utilized where the fluctuating velocity components  $u'$  that prevail during the lifetime of the turbulent eddy are sampled by assuming that they obey a Gaussian probability distribution, so that  $u' = \zeta \sqrt{u'^2}$ . Here  $\zeta$  is a normally distributed random number, and the remaining right-hand side is the local root mean square (RMS) velocity fluctuations can be obtained (assuming isotropy) by  $\sqrt{u'^2} = \sqrt{2k_g/3}$ . The interaction time between the particles and eddies is smaller of the eddy lifetime  $\tau_e$  and the particle eddy crossing time  $\tau_{cross}$ . The particle interacts with the fluid eddy over the interaction time. When the eddy lifetime is reached, a new value of the instantaneous velocity is obtained by applying a new value of  $\zeta$ .

### 3.3 Particle-wall collision model for Eulerian-Lagrangian model

The algebraic particle-wall collision model (Brach and Dunn, 1992 and 1998) and the stochastic wall roughness model (Sommerfeld, 1992) were implemented into the FLUENT code via the User-defined subroutines. This allows the flexibility for extending the collision model to handle complex engineering flows. In the algebraic particle-wall collision model, it is assumed that the majority of the energy loss due to deformation of particle and wall surface is lost during approach (establishment of contact), while the majority of energy loss due to molecular level forces, such as adhesion, is irreversible and occurs primarily during rebound (Brach and Dunn, 1998). Base on these assumptions, the kinematic restitution coefficient (overall restitution coefficient),  $e$ , can be expressed as:

$$e = -\frac{v_n^p}{u_n^p} = R_1(1 - \rho_1) \quad (3.72)$$

where  $u_n^p$  is the normal incident velocity and  $v_n^p$  is the normal reflected velocity.  $R_1$  presents the restitution coefficient in the absence of adhesion. And  $\rho_1$  denotes the adhesion coefficient that is defined as:

$$\rho_1 = -\frac{P_A^R}{P_D^A} \quad (3.73)$$

where  $P_A^R$  is the normal impulse due to adhesion during rebound and  $P_D^A$  is the normal impulse generated by deformation during approach. If  $\rho_1 = 1$ , the adhesion impulse completely counteracts the elastic restoring impulse, so the particle sticks on the wall. When  $\rho_1 = 0$ , there is, however, no energy loss due to adhesion, and the impact is equivalent to a macroimpact (Brach and Dunn, 1998).

Based on the above assumptions and the laws of impulse and momentum, the particle-wall collision model comprises of the following equations:

$$\begin{aligned} &\text{Error! Objects cannot be created from editing field codes.} \\ &\text{Error! Objects cannot be created from editing field codes.} \\ &\text{Error! Objects cannot be created from editing field codes.} \\ &\quad (3.74) \end{aligned}$$

where  $\mu_1$  is the ratio of tangential and normal impulse,  $\omega_p$  is the particle angular velocity before the collision and  $\Omega_p$  is the particle angular after collision. The above model allows the consideration of particle sliding or rolling throughout the contact duration on the surface. Under the sliding condition,  $\mu_1$  has the same value as the coefficient of friction. For the collision without sliding that the particle is rolling at the end of contact,  $\mu_1$  is given by:

$$\text{Error! Objects cannot be created from editing field codes.} \quad (3.75)$$

where  $\beta$  can be expressed as:

$$\text{Error! Objects cannot be created from editing field codes.} \quad (3.76)$$

The algebraic expressions for the impact coefficients based on (Brach and Dunn, 1998) will be experimentally determined through:

$$\text{Error! Objects cannot be created from editing field codes.} \quad (3.77)$$

$$\text{Error! Objects cannot be created from editing field codes.} \quad (3.78)$$

The constants  $k$ ,  $l$ ,  $a$ ,  $b$  and  $u_c$  (capture velocity or critical velocity) are to be obtained through experiments.

This study employed the roughness model developed by Sommerfeld, (1992) Here, the incident angle  $\theta'$  comprises of the particle incident angle  $\theta$  and a stochastic contribution due to the wall roughness, viz.,

$$\theta' = \theta + \gamma\xi \quad (3.79)$$

From the above,  $\xi$  is a Gaussian random variable with mean of 0 and a standard deviation of 1. The value of  $\gamma$ , which is dependent on the structure of the wall roughness and additionally on the particle sized (Sommerfeld and Huber, 1999), can be obtained through experiment.

When the absolute value of the negative  $\gamma\xi$  is larger than the incident angle, particles may not impact on the *lee* side of a roughness structure (See Figure 3.3). This so-called shadow effect leads to a higher probability for particles to collide on the *luff* side and a shift of the probability distribution function of  $\gamma\xi$  towards positive values. Sommerfeld and Huber (1999) pointed out that three regimes of the effective roughness angle distribution function can be identified for a given combination of  $\theta$  and  $\gamma$ :

- (i) The probability for particle to hit a roughness structure with  $|\gamma_+| > \theta$  is zero, i.e.  $f(\theta, \gamma) = 0$ .

- (ii) The probability for particle to hit a roughness structure with a negative inclination in the interval the interval  $0 < |\gamma_+| < \theta$  is smaller than that to hit the plane surface by the factor:  $f(\theta, \gamma) = \frac{\sin(\theta - \gamma)}{\sin \theta}$ .
- (iii) The probability to hit a positive inclined wall roughness structure is higher than to hit the plane surface by the facture:  $f(\theta, \gamma) = \frac{\sin(\theta - \gamma)}{\sin \theta}$ .

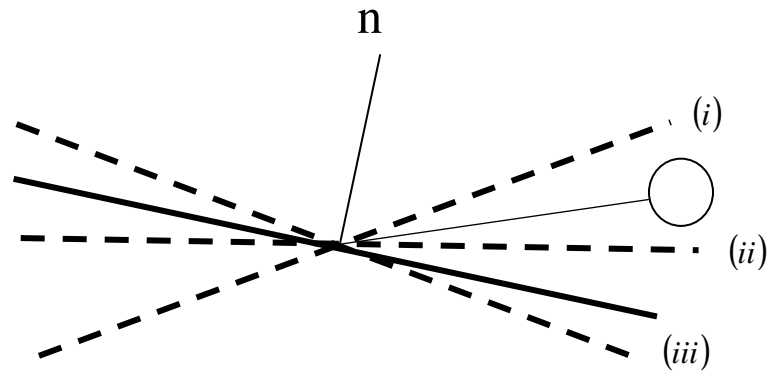


**Figure 3.3** Illustration of shadow effect due to wall roughness.

A program procedure proposed by Sommerfeld and Huber (1999) has been implemented to handle the shadow effect (Figure 3.4). In this procedure, the roughness angle  $\Delta\gamma^\xi$  is firstly sampled from a normal distribution function. If a negative roughness angle with an absolute value being larger than the particle incident angle  $\theta$  is sampled, an unphysical collision results, i.e. the particle would come behind the wall. Then, a new roughness angle is sampled (Sommerfeld and Huber, 1999). This procedure shifts the distribution function of  $\Delta\gamma^\xi$  towards the positive side and avoids the unphysical situation that particles hit the roughness structure with a negative angle.

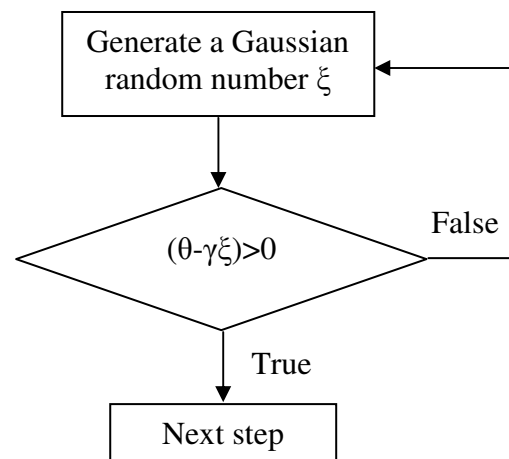


**Figure 3.4** Flowchart of the roughness wall model.